Notes

Conformational Studies of Paclitaxel Analogs Modified at the C-2′ Position in Hydrophobic and Hydrophilic Solvent Systems

Guillermo Moyna, Howard J. Williams, and A. I. Scott*

Center for Biological NMR, Department of Chemistry, Texas A&M University, College Station, Texas 77843-3255

Israel Ringel* and Raphael Gorodetsky

The Hebrew University−Hadassah Medical School, 12272 Jerusalem, Israel

Charles S. Swindell*

Department of Chemistry, Bryn Mawr College, 101 North Merion Avenue, Bryn Mawr, Pennsylvania 19010-2899

Received January 13, 1997[⊗]

The conformations of two paclitaxel analogs modified at the C-2′ position, 2′-deoxypaclitaxel and 2′-methoxypaclitaxel, were studied in hydrophobic and hydrophilic solvent systems by a combination of NMR spectroscopy, CD measurements, and molecular modeling. Both analogs have hydrophobic and hydrophilic conformations that resemble those of paclitaxel itself in the same media. Since the two have diminished biological activities in a number of bioactivity assays and the hydrogen-bonding capability of the 2′-hydroxyl group has been eliminated, we postulate that this group is involved in hydrogen bonding with tubulin and plays an important role in molecular recognition. The results of this study are in agreement with our earlier report on paclitaxel 2′-acetate, an analog in which the 2′-hydroxyl group hydrogen-bonding capacity has also been eliminated.

Introduction

Since its discovery 25 years ago,[1] the diterpene alkaloid paclitaxel (**1**) has become one of the most promising anticancer drugs, displaying activity against a variety of carcinomas, and it is presently used for the treatment of breast and ovarian cancers.[2] As opposed to other antimitotic drugs that destabilize microtubules, paclitaxel binds and stabilizes these cytoskeletal elements, preventing their reorganization into a functional mitotic spindle apparatus, inhibiting cell replication.[3] Added to this novel mode of action is a rich chemical functionality that permits fine tuning of biological activity and other pharmacological properties in rationally designed synthetic analogs.

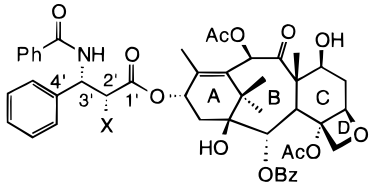

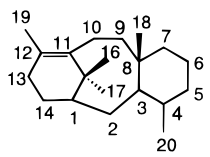

PACLITAXEL X = OH (1)

2'-METHOXYPACLITAXEL X = OMe (2)

2'-DEOXYPACLITAXEL X = H (3)

Although the structure−activity profile of paclitaxel has been extensively studied,[4−6] the conformation of the drug bound to microtubules has only been reported at low resolution.[7] The determination of this conformation is crucial for the development of synthetic analogs with improved bioactivity, and two models have been proposed to alleviate the lack of experimental data. One postulates a binding conformation resembling that of unbound paclitaxel in chloroform (hydrophobic) solution[8] and the other is based on the conformation observed in H_2O−DMSO (hydrophilic) solution.[9] In the hydrophobic model, the 3′-phenyl group points away from the diterpene moiety in a conformation similar to that of the crystalline analog Taxotere®,[9−11] while in the hydrophilic conformation the 3′-phenyl, 2-benzoate and the 4-acetate groups are clustered under the diterpene skeleton, in what is known as the "hydrophobically collapsed" conformation.[9,10]

The 2′-hydroxyl group was thought to stabilize paclitaxel's preferred binding conformation.[9] However, in a recent study we determined the conformations of the inactive paclitaxel analog paclitaxel 2′-acetate and found that both hydrophobic and hydrophilic conformations closely resembled those of the parent compound in the same solvent systems.[12] Since the 2′-hydroxyl is blocked in this analog, our findings indicate that this group is not necessary for conformational organization but must be involved in molecular recognition by microtubules, acting perhaps as a hydrogen bond donor in the microtubule−paclitaxel complex. The aim of the present study is to determine the conformations of two C-2′ paclitaxel analogs, 2′-methoxypaclitaxel (**2**) and 2′-deoxypaclitaxel (**3**), in which the hydrogen bonding capacity of the 2′-hydroxyl group has been eliminated, and correlate them with their paclitaxel-like biological activity. It complements our previous studies on the conformation of paclitaxel 2′-acetate and will aid in

[⊗] Abstract published in *Advance ACS Abstracts,* August 15, 1997.

S0022-2623(97)00026-5 CCC: $14.00

Scheme 1. Preparation of 2′-Methoxypaclitaxel (**2**) and 2′-Deoxypaclitaxel (**3**)

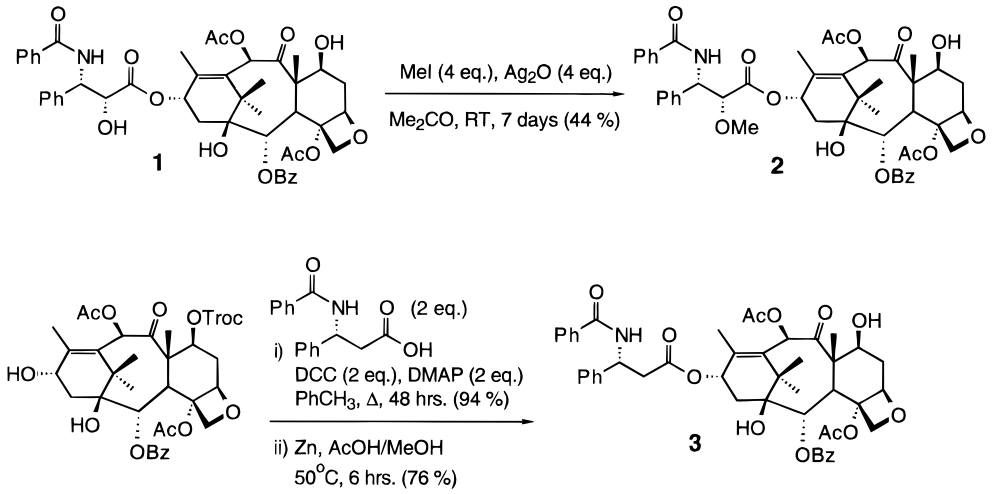

Table 1. NMR Data for 2′-Methoxypaclitaxel in $CDCl_3$ and DMSO−H_2O (Chemical Shifts Are Indicated in ppm and Coupling Constants in Hz)

^{1}H on	$CDCl_3$	DMSO−H_2O
C-2	5.66 (d, 7.1)	5.35 (d, 7.3)
C-3	3.77 (d, 7.1)	3.54 (d, 7.3)
C-5	4.93 (dd, 2.0, 9.8)	4.87 (dd, 2.2, 9.7)
C-6	2.52 (ddd, 6.8, 9.8, 15.1) α	2.31 (ddd, 6.4, 9.7, 14.6) α
	1.86 (ddd, 2.0, 10.9, 15.1) β	2.52 (ddd, 2.2, 10.8, 14.6) β
C-7	4.37 (bdd, 6.8, 10.9)	4.03 (dd, 6.4, 10.8)
C-10	6.25 (s)	6.21 (s)
C-13	6.27 (qdd, 1.0, 9.0, 9.2)	5.84 (qdd, 1.0, 9.1, 9.4)
C-14	2.33 (dd, 9.0, 15.3) α	2.14 (m) α and β
	2.18 (dd, 9.2, 15.3) β	
C-16	1.12 (s)	0.96 (s)
C-17	1.23 (s)	0.96 (s)
C-18	1.81 (d, 1.0)	1.72 (d, 1.0)
C-19	1.66 (s)	1.44 (s)
C-20	4.29 (d, 8.6) α	3.98 (m) α and β
	4.17 (d, 8.6) β	
C-2′	4.28 (d, 2.6)	4.30 (d, 9.2)
C-3′	5.70 (dd, 2.6, 8.9)	5.25 (d, 9.2)
C-3′-OMe	3.44 (s)	3.33 (s)
NH	7.08 (d, 8.9)	
OAc-10	2.20 (s)	2.06 (s)
OAc-4	2.38 (s)	2.16 (s)
OBz-*o*	8.10 (dd, 1.5, 8.0)	7.89 (dd, 1.3, 8.1)
OBz-*m*	7.50 (dd, 7.5, 8.0)	7.58 (dd, 7.5, 8.1)
OBz-*p*	7.60 (tt, 1.5, 7.5)	7.68 (tt, 1.3, 7.5)
NBz-*o*	7.75 (dd, 1.5, 8.1)	7.75 (dd, 1.4, 8.2)
NBz-*m*	7.38 (m)	7.43 (dd, 7.4, 8.2)
NBz-*p*	7.47 (tt, 1.5, 8.1)	7.51 (tt, 1.4, 7.4)
Ph-*o, m*	7.38 (m)	7.34 (m)
Ph-*p*	7.31 (tt, 1.6, 6.7)	7.12 (tt, 1.8, 6.6)

Table 2. NMR Data for 2′-deoxypaclitaxel in $CDCl_3$ and DMSO−H_2O (Chemical Shifts Are Indicated in ppm and Coupling Constants in Hz)

^{1}H on	$CDCl_3$	DMSO−H_2O
C-2	5.60 (d, 7.0)	5.40 (d, 7.2)
C-3	3.73 (d, 7.0)	3.63 (d, 7.2)
C-5	4.94 (dd, 2.0, 9.6)	4.90 (dd, 2.0, 9.6)
C-6	2.52 (ddd, 6.7, 9.6, 14.6) α	2.33 (ddd, 6.7, 9.6, 14.5)
	1.84 (ddd, 2.0, 11.0, 14.6) β	1.64 (ddd, 2.0, 10.8, 14.5)
C-7	4.35 (ddd, 4.1, 6.7, 11.0)	
C-10	6.19 (s)	6.23 (s)
C-13	6.10 (qdd, 1.2, 8.9, 8.9)	5.92 (qdd, 1.0, 8.9, 9.3)
C-14	2.16 (m) α and β	2.02 (m) α and β
C-16	1.08 (s)	0.97 (s)
C-17	1.15 (s)	0.97 (s)
C-18	1.63 (d, 1.2)	1.72 (d, 1.0)
C-19	1.48 (s)	1.46 (s)
C-20	4.27 (d, 8.5) α	4.00 (m) α and β
	4.12 (d, 8.5) β	
C-2′	3.19 (dd, 4.7, 16.0)	3.12 (dd, 8.0, 15.7)
	3.08 (dd, 5.6, 16.0)	3.01 (dd, 7.0, 15.7)
C-3′	5.73 (ddd, 4.7, 5.6, 8.6)	5.49 (dd, 7.0, 8.0)
NH	7.63 (d, 8.6)	
OAc-10	2.19 (s)	2.05 (s)
OAc-4	2.33 (s)	2.13 (s)
OBz-*o*	8.03 (dd, 1.4, 8.1)	7.91 (dd, 1.3, 8.2)
OBz-*m*	7.46 (dd, 7.6, 8.1)	7.52 (dd, 7.5, 8.2)
OBz-*p*	7.59 (tt, 1.4, 7.6)	7.64 (tt, 1.3, 7.5)
NBz-*o*	7.83 (dd, 1.6, 8.5)	7.75 (dd, 1.5, 8.4)
NBz-*m*	7.43 (dd, 7.6, 8.5)	7.42 (dd, 7.6, 8.4)
NBz-*p*	7.51 (tt, 1.6, 7.6)	7.50 (tt, 1.5, 7.6)
Ph-*o, m*	7.36 (m)	7.34 (m)
Ph-*p*	7.28 (m)	7.25 (tt, 1.3, 7.1)

further understanding the role of the 2′-hydroxyl group in the paclitaxel−microtubule complex.

Experimental Section

Preparation of C-2′ Analogs. 2′-Methoxypaclitaxel and 2′-deoxypaclitaxel were prepared as shown in Scheme 1, following the procedures of Kant[13] and Guéritte-Vogelein.[14] Paclitaxel and baccatin III necessary for the preparations were obtained from a mixture of paclitaxel and cephalomannine according to methods reported by Kingston.[15,16] NMR data for the compounds in the two solvent systems are reported in Tables 1 and 2. The HPLC retention times (RP18, MeOH: H_2O 65:35, 1 mL/min) are 19.3, 18.3 and 16.6 min for 2′-methoxypaclitaxel, 2′-deoxypaclitaxel, and paclitaxel, respectively, which indicates that the hydrophobicity of the two analogs is roughly comparable to that of paclitaxel.

Microtubule Assembly Assays. Calf brain microtubule protein (MTP) was purified by two cycles of temperature dependent assembly−disassembly following reported procedures.[17] Microtubule assembly in the presence and absence of drugs was monitored spectrophotometrically at 35 °C, and changes in turbidity (representative of polymer mass) were monitored at 350 nm.[18]

(a) Effect of 2′-Analogs on Cell Proliferation. The effect of the analogs was tested on three cell lines: Murine macrophage-like cells (J774.2) were received from Dr. S. B. Horwitz (Albert Einstein College of Medicine, New York) and maintained in DMEM medium supplemented by 10% horse serum, antibiotics, and glutamine.[19] Murine mammary adenocarcinoma cells (EMT-6) were maintained in Waymouths medium supplemented by 15% FCS, antibiotics, and glutamine.[20] Human ovarian carcinoma cells (OV-1063) were isolated from an ovarian tumor and established as a line by Dr. A. T. Horowitz at Hadassah University Hospital, Jerusalem. The cells were grown in RPMI-1640 medium supplemented by 10% FCS, antibiotics, and glutamine.[21] All cells were platted in wells and incubated with a range of drug concentrations and the number of viable cells in each well was determined after 72 h utilizing Coulter counter or the MTS colorimetric assay.

(b) Microtubule Bundle Formation in Cells. Human fibrosarcoma cells (HT 1080) were incubated for 4 h with high

concentration of paclitaxel (1 μM), 2′-methoxypaclitaxel (5 μM), and 2′-deoxypaclitaxel (5 μM). Treated cells were analyzed for changes in microtubule structures using inmunofluorescence anti-tubulin antibodies.

NMR Experiments. ^{1}H NMR spectroscopy was performed on a Bruker ARX-500 operating at 500 MHz, using either ^{1}H-BB inverse or HCN probes. For 1D spectra 32K data points were used, while 2D spectra were recorded with matrix sizes of 2K × 0.5K. A 600 ms hard pulse spin lock was used for ROESY experiments.[22] Solvent suppression in the H_2O containing samples was by presaturation. Samples were dissolved in $CDCl_3$ or d_6-DMSO−H_2O (1:1) to a final concentration of 10 or 2 mM respectively. The residual solvent peak (7.24 ppm for $CHCl_3$ and 2.49 ppm for DMSO) was used for spectral calibration. Spectra were recorded at 295 K for $CDCl_3$ samples and at 310 K for d_6-DMSO−H_2O samples.

Circular Dichroism Measurements. Near-UV circular dichroism (CD) spectra of 1×10^{-4} M $CHCl_3$ and DMSO−H_2O (1:1) solutions of paclitaxel, 2′-methoxypaclitaxel, and 2′-deoxypaclitaxel were collected at 25 °C with an AVIV 62DS CD spectrometer using a 0.1 cm quartz cell. A bandwidth of 0.5 nm, a time constant of 1 s, and a step size of 0.5 nm were employed. For each sample, three scans from 350 to 250 nm were recorded and averaged. Further processing included subtraction of the solvent background spectra obtained under identical conditions and three-point smoothing of the resulting data.

Molecular Modeling. All molecular modeling was performed using Sybyl 6.3 (Tripos Associates Inc.) running on a Silicon Graphics Iris Indigo R4000 workstation. The Tripos 6.0 force field with Gasteiger−Hückel charges was used for all energy evaluations.[23,24] An energy gradient of 0.05 kcal/mol was used as termination criteria in geometry optimizations. Starting structures for all modeling experiments were based on the Taxotere® crystal structure coordinates.[11]

Grid searching around the C2′−C3′ bond was performed by rotating the <C1′−C2′−C3′−C4′> dihedral angle in 10° steps over the 360° rotation range to analyze possible conformations for the two 2′-position analogs side chains.[25] For each rotamer, the dihedral angle was held fixed while the geometry of the rest of the molecule was optimized. No NMR derived restraints were used in these simulations.

Sets of low-energy conformers for both analogs were obtained by restrained simulated annealing.[26,27] Distance range constraints were obtained from the ROESY cross-peaks and classified according to peak area into strong (1.8−2.7 Å), medium (1.8−3.3 Å), and weak (1.8−5.0 Å). When appropriate, dihedral angle constraints were derived from the ^{1}H coupling constants obtained from the 1D spectra using the Karplus equation,[28] without consideration of substituent effects. Structure sets were obtained by 100 cycles of simulated annealing, each consisting of heating at 800 K for 1000 fs, followed by exponential annealing to 200 K for 1000 fs and subsequent energy minimization. Energy penalties of 200 kcal/Å^2 and 0.05 kcal/deg^2 were applied for violations of range and dihedral angle constraints respectively in the simulations. The ten lowest energy conformers from the sets were used for structural comparison. Superposition and root mean square deviation (RMSD) calculations on the final structure sets was done using software previously developed in our lab.[29]

Dynamic simulations on low-energy conformers obtained from restrained simulated annealing consisted of a 100 ps equilibration period at 298 K, followed by a 1000 ps structure analysis period at the same temperature. Conformations were sampled at 100 fs intervals, while nonbonded interactions were updated every 25 fs. The 10 000 conformers obtained were used to study the mobility of the side chain substituents.

Results

Biological Studies. (a) Microtubule Assembly. As shown in Figure 1, both compounds are weaker promoters of microtubule polymerization than paclitaxel. For solutions of 1 mg/mL of microtubule protein, the initial assembly slope after time lag compared to the initial assembly slope of paclitaxel was 0.21 and 0.33 for 2′-methoxypaclitaxel and 2′-deoxypaclitaxel, respectively. Normal microtubules were observed by electron microscopy (data not shown).

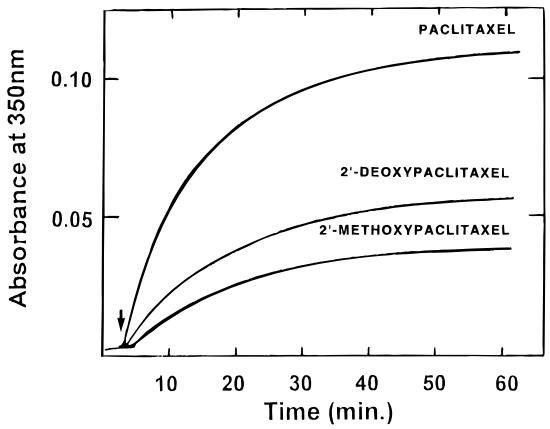

Figure 1. Assembly of MTP in the presence of 2′-methoxypaclitaxel, 2′-deoxypaclitaxel, and paclitaxel. A 1 mg/mL solution of MTP was incubated at 35 °C, and at the time, denoted by an arrow, 10 μM drug was added. The assembly reactions were followed by turbidity measurements at 350 nm.

Table 3. Sensitivity of J774.2, EMT-6, and OV-1063 Cells to 2′-Analogs Compared to Paclitaxel (IC_{50}, Drug Concentration That Inhibits Cell Proliferation by 50% after 72 h)

	IC_{50} (μM)		
drug	J774.2	EMT-6	OV-1063
paclitaxel	0.015	0.009	0.015
2′-methoxypaclitaxel	0.47	0.27	0.27
2′-deoxypaclitaxel	0.40	0.30	0.45

(b) Effect of 2′-Analogs in Cell Proliferation. Both analogs were, on average, at least 30 times less active than paclitaxel in inhibiting cell proliferation on the three cell lines studied. These results are summarized in Table 3. Similar activity for the two analogs has been reported on other cell lines.[13]

(c) Microtubule Bundle Formation in Cells. Results from inmunofluorescence studies on HT 1080 cells are shown in Figure 2. Paclitaxel-treated cells presented bundles of microtubules, while cells treated with a 5-fold higher concentration of 2′-methoxypaclitaxel and 2′-deoxypaclitaxel differed little from untreated cells.

Conformational Studies. (a) Circular Dichroism Studies. As reported by Balasubramanian *et al.*,[30,31] the CD spectrum of paclitaxel can be used to probe conformational changes arising from effects of solvent polarity. The broad negative absorption near 300 nm due to $\pi-\pi^*$ transitions of the aromatic groups shifts to shorter wavelengths with increasing solvent polarity, indicating a rotation around the C2′−C3′ bond. Paclitaxel showed an absorption shift from 303 to 296 nm when going from $CHCl_3$ to DMSO−H_2O (1:1), in good agreement with the published data.[30] For the same solvent systems, the observed shifts in absorption were from 304 to 294 nm for 2′-methoxypaclitaxel and from 303 to 294 nm for 2′-deoxypaclitaxel, almost identical in both cases to the absorption shift seen for paclitaxel.

(b) Identification of Low-Energy C2′−C3′ Rotamers. Several studies indicate that the major conformational change undergone by taxoids in response to polarity of solvent involves rotation around the C2′−

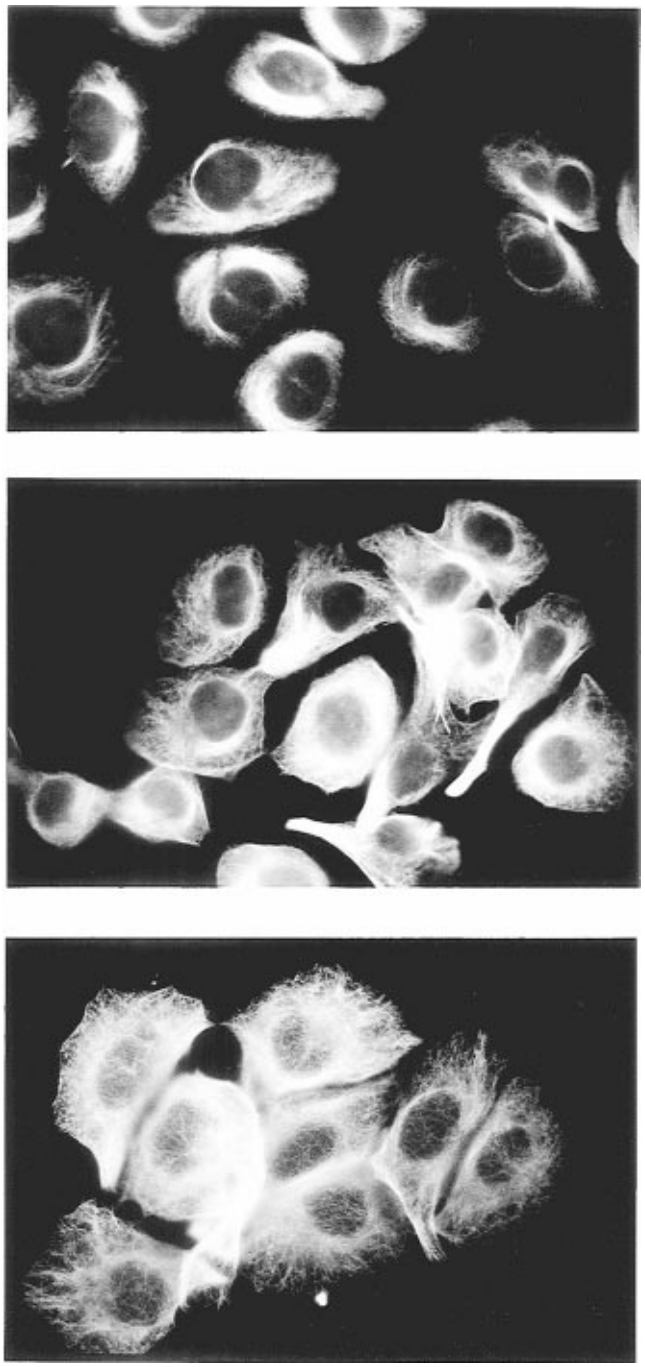

Figure 2. Microtubule bundle formation in human fibrosarcoma cells. Inmunofluorescence shows that cells treated with high concentration of paclitaxel (**a**, top) present microtubule bundles, while cells treated with high concentration of either 2′-methoxypaclitaxel or 2′-deoxypaclitaxel (**b**, center and **c**, bottom, respectively) presented small changes from untreated cells.

C3′ bond.[8−10,12,29−31] 2′-Methoxypaclitaxel, with a somewhat bulkier group in the 2′-position, would be expected to have a similar behavior. The coupling constants found for this compound in hydrophobic and hydrophilic solvents (Table 1) are comparable to those found for paclitaxel in the same media, suggesting that the conformational changes are indeed similar. On the other hand, the analysis of 2′-deoxypaclitaxel is complicated by several factors. Since no substituents are present at the 2′-position, a higher freedom of rotation of the C2′−C3′ bond can be expected. Evidence of this is the observed coupling constant values of the C2′ and C3′ protons in both solvent system for this compound (Table 2), which indicate that at room temperature ^3J couplings are affected significantly by rotational averaging.[32] A second problem is the difficulty in making unambiguous assignments of the diastereotopic protons at C2′, which precludes the use of ROESY correlations and coupling constants in modeling. For these reasons, an identification of low-energy rotamers around C2′−C3′ was carried out by grid searching for both 2′-position analogs and compared to the energy profile around the same bond for paclitaxel. All compounds presented profiles with two distinct minima. For paclitaxel they were found at <C1′−C2′−C3′−C4′> dihedral angles of 140° and −70°. In 2′-methoxypaclitaxel the low-energy rotamers had <C1′−C2′−C3′−C4′> dihedral angles of 150° and −70°. These values correlate well with those previously reported for low-energy conformations obtained by Monte Carlo searching of paclitaxel and 2′-acetylpaclitaxel.[10,12] The energy profile of 2′-deoxypaclitaxel showed minima at <C1′−C2′−C3′−C4′> dihedral angles of 160° and −60°, closely resembling the results obtained for taxoids with electronegative 2′-substituents.

(c) Generation of Low-Energy Structures by Restrained Simulated Annealing. Sets of hydrophobic and hydrophilic solution structures for both compounds were generated by simulated annealing as described in the Experimental Section. Distance range constraints derived from ROESY spectra and dihedral angle constraints from dipolar coupling information were included in the simulations to obtain low-energy structure sets in agreement with the NMR data.

The ROESY spectrum of 2′-methoxypaclitaxel in hydrophilic solution indicates that there is a close contact between the side chain 2′, 3′ and 3′-*o*-phenyl protons and the 4-acetate methyl protons. NOE interactions between the 2-*o*-benzoate protons and the 4-acetate methyl protons reveal a clustering of the aromatic groups under the diterpene moiety. The coupling constant of protons H2′-H3′ is 9.2 Hz, indicating a <H3′−C3′−C2′−H2′> dihedral angle of 175 ± 5°. This is indicative of an anti configuration of the side chain substituents and is in agreement with the low-energy rotamer with <C1′−C2′−C3′−C4′> dihedral of −70° found in the grid search. Weaker NOE signals between the side chain protons and the 4-acetate methyl protons are present in hydrophobic solution. The prominent NOE cross-peak arising from the interaction of 3′-*o*-phenyl proton to the 4-acetate methyl protons observed in hydrophilic solution is only detectable at very low contour levels of the 2D spectrum in this case. This can be explained by a greater interaction of the side chain 3′-phenyl with the solvent and less clustering of the hydrophobic groups. An H2′−H3′ coupling constant of 2.6 Hz indicates that the dihedral angle <H3′−C3′−C2′−H2′> is 55 ± 5° in this case, in agreement with a gauche configuration of the side chain substituents and consistent with the grid search low-energy rotamer with <C1′−C2′−C3′−C4′> dihedral of 150° described earlier. Superpositions of ten low-energy structures of 2′-methoxypaclitaxel in hydrophilic and hydrophobic solution are shown in Figure 3. The set of hydrophilic solution structures used in the superposition were within 1.8 kcal/mol of the global minima and had a RMSD of 0.54 ± 0.03 Å. The energy range was within

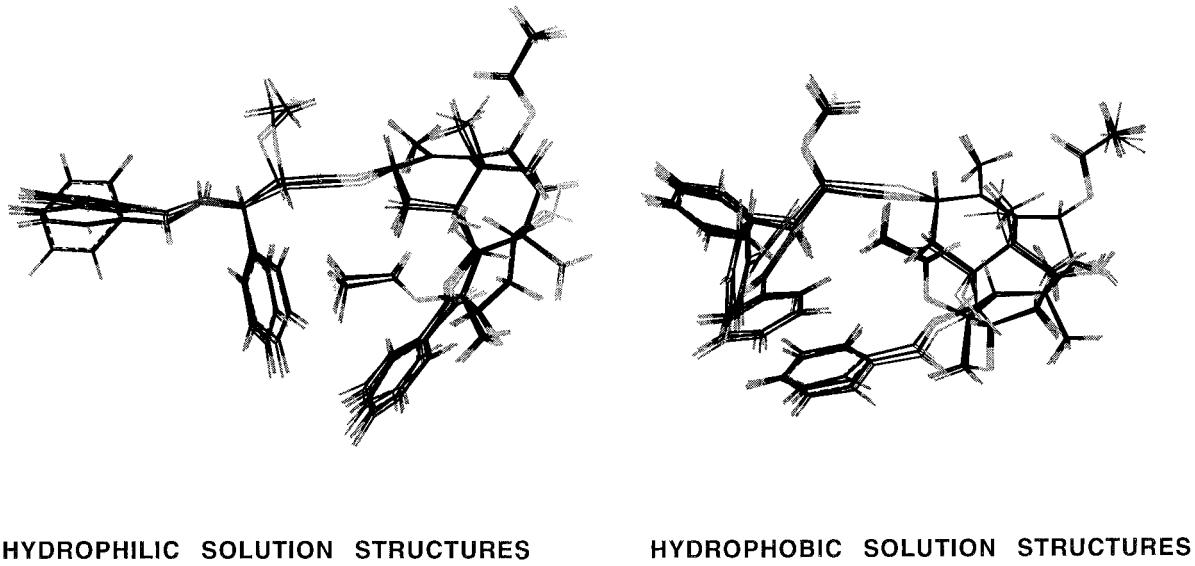

Figure 3. Superposition of ten low-energy conformers of 2′-methoxypaclitaxel in hydrophilic and hydrophobic solvent.

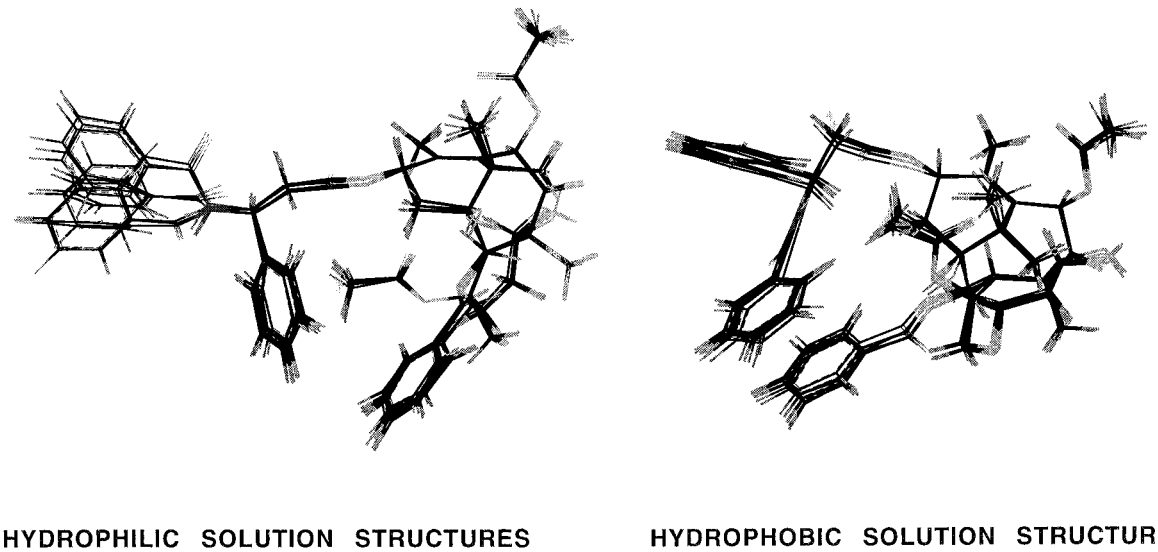

Figure 4. Superposition of ten low-energy conformers of 2′-deoxypaclitaxel in hydrophilic and hydrophobic solvent.

2.7 kcal/mol of the global minima for the hydrophobic solution set, and the RMSD of the set was 0.52 ± 0.03 Å. Due to the lack of significant NOE signals, the 3′-benzamide atoms were not considered in the superposition and RMSD calculations in either case.

NOE signals indicate proximity between the 3′ and 3′-*o*-phenyl side chain protons and the 4-acetate methyl protons of 2′-deoxypaclitaxel in hydrophilic solution. There are also ROESY correlation to both of the 2′ protons. Since their identities cannot be unambiguously determined, a pseudoatom was used to represent the diastereotopic protons when defining distance range constraints. NOE correlations from the 2-*o*-benzoate protons to the 4-acetate indicate that the aromatic groups are clustered in aqueous solutions of this analog, as was found for 2′-methoxypaclitaxel. The coupling constants from the protons at C2′ to proton H3′, 7.0 and 8.0 Hz, indicate possible rotational averaging, and therefore no dihedral angle constraints were used in the generation of the conformer set. The hydrophobic solution ROESY spectra of 2′-deoxypaclitaxel also shows weaker interactions between the side chain protons and the 4-acetate protons, indicating, as for 2′-methoxypaclitaxel, greater interaction of the side chain 3′-phenyl with the solvent and less clustering of hydrophobic groups in hydrophobic media. Coupling constants of 5.6 and 4.5 Hz were found from the C3′ protons to the H2′ proton in this case, again indicating possible averaging and preventing the use of this information for determining dihedral angle constraints. Superpositions of ten low-energy structures of 2′-deoxypaclitaxel in hydrophilic and hydrophobic solution are shown in Figure 4. The energy of the hydrophilic solution structures used in the superposition were within 2.1 kcal/mol of the global minima, and the RMSD of the set was 0.42 ± 0.02 Å. The energy range for the hydrophobic solution structure set was within 2.7 kcal/mol of the local minima, and the set had an RMSD of 0.38 ± 0.02 Å. As was the case for 2′-methoxypaclitaxel, the 3′-benzamide atoms were not considered in the superposition and RMSD calculations in either case due to the lack of significant NOE signals. It is worth noticing that the average <C1′−C2′−C3′−C4′> dihedral angles of the hydrophobic and hydrophilic structure sets are, respectively, 170 ± 5° and −70 ± 5°, in agreement with the <C1′−C2′−C3′−C4′> dihedral angle values of low-energy rotamers of 2′-deoxypaclitaxel found in the grid search. These torsions indicate anti and gauche ar-

rangements of the side chain substituents in hydrophilic and hydrophilic media, respectively, as was found for 2′-methoxypaclitaxel and for paclitaxel and other paclitaxel analogs studied previously.

(d) Dynamics of Hydrophobic and Hydrophilic Models. Low-energy conformers obtained by restrained simulated annealing were subjected to dynamic simulations to evaluate the local mobility of the side chains at room temperature. In all models, the 3′-benzamide phenyl ring underwent several full rotations in the time period analyzed, and the atoms of this group had the highest average RMSD when compared to the rest of the molecule, indicating high local mobility. When the simulations of the two 2″-position analogs were compared, higher rotational freedom was observed for the protons of the C2′−C3′ bond in both 2′-deoxypaclitaxel models. In hydrophilic simulations, the $<H2'_{pro-R}-2'-C3'-H3'>$ and $<H2'_{pro-S}-C2'-C3'-H3'>$ dihedral angles in 2′-deoxypaclitaxel were $-70 \pm 31°$ and $173 \pm 31°$ respectively, while the <H2′−C2′−C3′−H3′> dihedral angle was $174 \pm 10°$ in 2′-methoxypaclitaxel. In hydrophobic simulations, the dihedral angles were, in the same order, $166 \pm 36°$ and $46 \pm 36°$ in 2′-deoxypaclitaxel and $54 \pm 10°$ in 2′-methoxypaclitaxel.

Discussion

CD measurements, grid searching, and NMR-restrained simulated annealing experiments indicate that both analogs studied take on solution conformations similar to those of paclitaxel and other analogs previously studied in similar media. The lack of NOE correlations from the C3′-benzamide phenyl protons to the rest of the molecule in the cases studied could be explained by the high mobility of this group, as demonstrated by the dynamic simulations. Further evidence of this dynamic behavior was recently reported in an elegant study by Ojima *et al.*, who used temperature effects on ^{19}F chemical shifts to study the conformations of paclitaxel, Taxotere®, and paclitaxel 2′-acetate analogs fluorinated on side chain aromatic rings.[33] In the case of 2′-deoxypaclitaxel models, the dynamic experiments also indicate that ^3J coupling averaging would occur at room temperature due to the higher rotational freedom of the side chain lacking 2′-substituents.

Neither removal of paclitaxel's 2′-OH nor its modification to a methoxy group significantly affects the conformations in the two-solvent systems studied, indicating that the 2′-OH does not stabilize a particular solution structure and in fact its modification has almost no effect on conformation. However, a substantial decrease in biological activity is encountered for both analogs studied. As the 2′-OH group with the proper stereochemistry is necessary for full activity, its action must not occur through intramolecular hydrogen bonding stabilizing an active conformation of the drug but rather through interaction with the microtubule binding site, perhaps by hydrogen bonding to polar amino acid residues, insertion into a polar pocket of the site, or interaction with water bound to the protein. The findings reported here are in good agreement with our previous studies on the conformations of 2′-acetylpaclitaxel, an inactive 2′-position analog.[12] Further studies designed to determine the mode of binding of paclitaxel in paclitaxel−microtubule complexes are underway.

Acknowledgment. Financial support from the NIH through Grant GM32596 and funding from the Texas Advanced Technology Research Program are gratefully acknowledged (A.I.S.). Support from the Hebrew University Medical Research Fund is also acknowledged (I.R.). We also thank Dr. Paul W. Baures, Mr. Hilal A. Lashuel, and Dr. Jeffery W. Kelly for their assistance with the CD experiments.

References

(1) Wani, M. C.; Taylor, H. L.; Wall, M. E.; Coggon, P.; McPhail, A. T. Plant antitumor agents VI. The isolation and strucutre of taxol, a novel antileukimic and antitumor agent from *Taxus brevifolia*. *J. Am. Chem. Soc.* **1971**, *93*, 2325−2327.

(2) Arbuck, S. G.; Blaylock, B. A. Taxol: clinical results and current issues in development. In *Taxol:® Science and Applications*; Suffnes, M., Ed.; CRC Press: Boca Raton, FL, 1995; Chapter 14.

(3) Schiff, P. B.; Fant, J.; Horwitz, S. B. Promotion of microtubule assembly *in vitro* by taxol. *Nature (London)* **1979**, *277*, 665−667.

(4) Chen, S. H.; Farina, V. Paclitaxel (taxol®) chemistry and structure activity relationships. In *The Chemistry and Pharmacology of Taxol® and its Derivatives;* Farina, V., Ed.; Elsevier Science B. V.: Amsterdam, 1995; Chapter 5.

(5) Georg, G. I.; Boge, T. C.; Cheruvallath, Z. S.; Clowers, J. S.; Harriman, G. C. B.; Hepperle, M.; Park, H. The medicinal chemistry of taxol. In *Taxol:® Science and Applications*; Suffnes, M., Ed.; CRC Press: Boca Raton, FL, 1995; Chapter 13.

(6) Georg, G. I.; Harriman, G. C. B.; Vander Velde, D. G.; Boge, T. C.; Cheruvallath, Z. S.; Datta, A.; Hepperle, M.; Park, H.; Himes, R. H.; Jayasinghe, L. Medicinal chemistry of paclitaxel: Chemistry, structure-activity relationships, and conformational analysis. In *Taxane Anticancer Agents. Basic Science and Current Status;* Georg, G. I., Chen, T. T., Ojima, I., Vyas, D. M., Eds.; ACS Symposium Series 583; American Chemical Society: Washington, DC, 1994; Chapter 16.

(7) Nogales, E.; Wolf, S. G.; Khan, I. A.; Luduena, R. F.; Downing, K. H. Structure of tubulin at 6.5 Å and location of the taxol-binding site. *Nature (London)* **1995**, *375*, 424-427.

(8) Williams, H. J.; Scott, A. I.; Dieden, R. A.; Swindell, C. S.; Chirlian, L. E.; Francl, M. M.; Heerding, J. M.; Krauss, N. E. NMR and molecular modeling study of active and inactive taxol analogs in aqueous and non-aqueous solution. *Can. J. Chem.* **1994**, *72*, 252−260.

(9) Vander Velde, D. G.; Georg, G. I.; Grunewald, G. L.; Gunn, C. W.; Mitscher, L. A. "Hydrophobic collapse" of taxol and Taxotere solution conformations in mixtures of water and organic solvent. *J. Am. Chem. Soc.* **1993**, *115*, 11650−11651.

(10) Williams, H. J.; Scott, A. I.; Dieden, R. A.; Swindell, C. S.; Chirlian, L. E.; Francl, M. M.; Heerding, J. M.; Krauss, N. E. NMR and molecular modeling study of the conformations of taxol and ist side chain methyl ester in aqueous and non-aqueous solution. *Tetrahedron* **1993**, *49*, 6545−6560.

(11) Guéritte-Vogelein, F.; Guénard, D.; Mangatal, L.; Potier. P.; Guilhem, J.; Cesario, M.; Pascard, C. Structure of a synthetic taxol precursor: *N-tert*-butoxycarbonyl-10-deacetyl-*N*-debenzoyltaxol. *Acta Crystallogr.* **1990**, *C46*, 781−784.

(12) Williams, H. J.; Moyna, G.; Scott, A. I.; Swindell, C. S.; Chirlian, L. E.; Heerding, J. M.; Williams, D. K. NMR and molecular modeling study of the conformations of taxol 2′-acetate in chloroform and aqueous dimethylsulfoxide solutions. *J. Med. Chem.* **1996**, *39*, 1555−1559.

(13) Kant, J.; Huang, S.; Wong, H.; Fairchild, C.; Vyas, D.; Farina, V. Studies toward structure-activity relationships of Taxol®-SPCLN synthesis and cytotoxicity of Taxol® analogues with C-2′ modified phenylisoserine side chains. *BioMed. Chem. Lett.* **1993**, *3*, 2471-2474.

(14) Guéritte-Vogelein, F.; Guénard, D.; Le Goff, M-T.; Mangatal, L.; Potier, P. Relationships between the structure of taxol analogues and their antimitotic activity. *J. Med. Chem.* **1991**, *34*, 992−998.

(15) Rimoldi, J. M.; Molinero, A. A.; Chordia, M. D.; Gharpure, M. M.; Kingston, D. G. I. An improved procedure for the separation of paclitaxel and cephalomannine. *J. Nat. Prod.* **1996**, *59*, 167−168.

(16) Magri, N. F.; Kingston, D. G. I.; Jitrangsri, C.; Piccariello, T. Modified taxols. 3. Preparation and acylation of Baccatin III. *J. Org. Chem.* **1986**, *51*, 3239−3242.

(17) Ringel, I.; Horwitz, S. B. Taxol is converted to 7-epitaxol, a biologically active isomer, in cell culture medium. *J. Pharm. Ther.* **1987**, *242*, 692−698.

(18) Gaskin, F.; Cantor, C. R.; Shelanski, M. L. Turbidometric studies of the *in vitro* assembly and disassembly of porcine microtubules. *J. Mol. Biol.* **1974**, *89*, 737−758.

(19) Roy, S. N.; Horwitz, S. B. A phosphoglycoprotein associated with taxol resistance in J774.2 cells. *Cancer Res.* **1985**, *45*, 3856−3863.
(20) Rockwell, S. Cytotoxic and radiosensitizing effect of hypoxic sensitizers on EMT-6 mouse mammary tumor cells *in vivo* and *in vitro*. *Br. J. Cancer* **1978**, *37*, 212−215.
(21) Horowitz, A. T.; Treves, A. J.; Voss, R.; Okon, E.; Fuks, Z.; Davidson, L.; Biran, S. A new human carcinoma cell line: Establishment and analysis of tumor associated markers. *Oncology* **1985**, *42*, 332−337.
(22) Kessler, H.; Griesinger, C.; Kerssebaum, R.; Wagner, K.; Ernst, R. R.; Separation of cross-relaxation and J cross peaks in 2D rotating-frame NMR spectroscopy. *J. Am. Chem. Soc.* **1987**, *109*, 607−609.
(23) Clark, M.; Cramer, R. D.; Van Opdenbosch, N. Validation of the general purpose Tripos 5.2 force field. *J. Comput. Chem.* **1989**, *10*, 982−1012.
(24) Burkert, U.; Allinger, N. L. *Molecular Mechanics*, ACS Monograph 177; American Chemical Society: Washington, DC, 1982.
(25) Marshall, G. R.; Barry, C. D.; Bosshard, H. E.; Dammkoehler, R. A.; Dunn, D. A. The conformational parameter in drug design: The active analog aproach. In *Computer-Assisted Drug Design*; Olson, E. C., Christoffersen, R. E., Eds.; ACS Symposium Series 112; American Chemical Society: Washington, DC, 1979; Chapter 9.
(26) Brünger, A. T.; Clore, G. M.; Gronenborg, A. M., Karplus, M. Solution conformations of human growth hormone releasing factor: Comparison of the restained molecular dynamics and distance geometry methods for a system without long-range distance data. *Protein Eng.* **1987**, *1*, 399−406.
(27) Nigles, M.; Clore, G. M.; Gronenborn, A. M. Determination of three-dimansional structures of proteins from interproton distance data by hybrid distance geometry-dynamical simulated annealing calculations. *FEBS Lett.* **1988**, *229*, 317−324.
(28) Karplus, M. Vicinal proton coupling in nuclear magnetic resonance. *J. Am. Chem. Soc.* **1963**, *85*, 2870−2871.
(29) Moyna, G.; Mediwala, S.; Williams, H. J.; Scott, A. I. A simple algorithm for superimposing sets of NMR derived structures: Its application to the conformational study of cephalomannine in lipophobic and lipophilic systems. *J. Chem. Inf. Comput. Sci.* **1996**, *36*, 1224−1227.
(30) Balasubramanian, S. V.; Alderfer, J. L.; Straubinger, R. M. Solvent- and concentration-dependent molecular interactions of taxol (Paclitaxel). *J. Pharm. Sci.* **1994**, *10*, 1470-1476.
(31) Balasubramanian, S. V.; Straubinger, R. M. Taxol-lipid interactions: Taxol-dependent effects on physical properties of model membranes. *Biochemistry* **1994**, *33*, 8941−8947.
(32) Karimi-Nejad, Y.; Schmidt, J. M.; Rüterjans, H.; Schwalbe, H.; Griesinger, C. Conformation of valine side chains in ribonuclease T_1 determined by NMR studies of homonuclear and heteronuclear ^3J coupling constants. *Biochemistry* **1994**, *33*, 5481−5492.
(33) Ojima, I.; Kuduk, S. D.; Chakravarty, S.; Ourevitch, M.; Bégué, J.-P. A novel approach to the study of solution structures and dynamic behavior of paclitaxel and docetaxel using fluorine-containing analogs as probes. *J. Am. Chem. Soc.* **1997**, *119*, 5519−5527.

JM970026+